

# Hydrogen-Bond-Donating Acidity and Dipolarity/Polarizability of Surfaces within Silica Gels and Mesoporous MCM-41 Materials

Stefan Spange,\* Yvonne Zimmermann, and Annett Graeser

Department of Polymer Chemistry, Institute for Chemistry, University of Technology Chemnitz, Strasse der Nationen 62, D-09107 Chemnitz, Germany

Received May 19, 1999. Revised Manuscript Received August 4, 1999

Linear solvation energy (LSE) relationships are employed to characterize the internal polarities in the channels of a siliceous MCM-41 material and of a silica gel synthesized by a sol–gel process from tetramethoxysilane (TMOS). The polarity of the surfaces inside the silica gel and the mesopores of the MCM-41 can be quantitatively described by three independent terms: the dipolarity/polarizability ( $\pi^*$ ), the HBD (hydrogen-bond-donating) acidity ( $\alpha$ ), and the HBA (hydrogen-bond-accepting) ability ( $\beta$ ). These terms are defined by means of the Kamlet–Taft solvent parameters  $\alpha$ ,  $\beta$ , and  $\pi^*$  as a reference system. The following indicators have been encapsulated by the sol–gel process within the silica matrix or adsorbed to MCM-41: 2,6-diphenyl-4-(2,4,6-triphenyl-1-pyridinio)phenolate (**1**), dicyanobis-(1,10-phenanthroline)iron(II) (**2**), and Michler's ketone (**3**). The solvatochromic UV/vis spectroscopic band shifts of these indicators correlate with the Kamlet–Taft solvent parameters  $\alpha$  and  $\pi^*$ . The hydrogen-bond-donating acidity,  $\alpha$ , within MCM-41 increases significantly with decreasing temperature, whereas the dipolarity/polarizability term,  $\pi^*$ , is temperature-independent. With **2** as indicator, an average hydrogen-bond acidity ( $\alpha$ ) is measured, whereas **3** is suitable to distinguish between differently acidic silanols within MCM-41 as shown by surface titration of the adsorbed indicator **3** with a sterically hindered base.

## Introduction

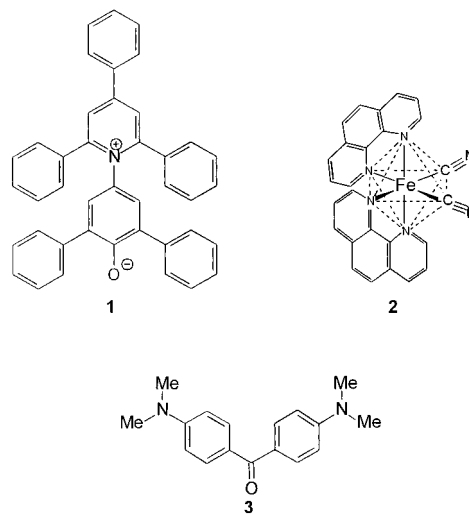
In two recent papers, the internal surface polarities inside a hexagonal ordered mesoporous siliceous host material, such as MCM-41 (Mobil code)<sup>1</sup> and silica gels,<sup>1,2</sup> synthesized by a sol–gel process, were examined by means of different fluorescence-active probe molecules such as *N,N*-dimethyl-1-naphthylamine (DMNA)<sup>1</sup> or pyrene.<sup>2</sup> DMNA was used because its UV/vis fluorescence maximum, measured in different environments,<sup>3</sup> correlates well with Reichardt's  $E_T(30)$  solvent polarity parameter.<sup>4</sup> The well-established  $E_T(30)$  polarity parameter is defined as the molar transition energy of Reichardt's dye **1** [2,6-diphenyl-4-(2,4,6-triphenyl-1-pyridinio)phenolate] (see Scheme 1), expressed as kilocalories per mole ( $\text{kcal mol}^{-1}$ ) (eq 1), dissolved in the solvent of choice. The dimensionless normalized  $E_T^N$  scale was later recommended to circumvent the obsolete energy unit kilocalories per mole ( $\text{kcal mol}^{-1}$ ).<sup>5</sup> It is defined according to eq 2, using water ( $E_T^N = 1$ ) and tetramethylsilane ( $E_T^N = 0$ ), respectively, as extreme polar and nonpolar reference solvents.

$$E_T(30) [\text{kcal mol}^{-1}] = (2.8591 \times 10^{-3}) \nu_{\text{max}}(\mathbf{1}) [\text{cm}^{-1}] \quad (1)$$

$$E_T^N = [E_T(30) - 30.7]/32.4 \quad (2)$$

Accordingly, the surface polarity in the narrow, controlled pore size channels of MCM-41 and inside

## Scheme 1. Formulas of the Probe Dyes Used



silica gels can be classified in relation to the corresponding  $E_T(30)$  solvent polarity scale as reference system.

(1) Ohtaki, M.; Inata, K.; Eguchi, K. *Chem. Mater.* **1998**, *10*, 2582–2584.

(2) Baker, G. A.; Jordan, J. D.; Bright, F. V. *J. Sol-Gel Sci. Technol.* **1998**, *11*, 43–54.

(3) Seliskar, C. J.; Brand, L. *J. Am. Chem. Soc.* **1971**, *93*, 5414.

(4) Dimroth, K.; Reichardt, C.; Siepmann, T.; Bohlmann, F. *Justus Liebigs Ann. Chem.* **1963**, 661, 1.

(5) Reichardt, C.; Harbusch-Görnert, E. *Justus Liebigs Ann. Chem.* **1983**, 721.

Ohtaki et al.<sup>1</sup> have shown that the surface polarity inside a silica gel [ $E_T^N = 0.9$  from ref 1,  $E_T(30) = 59.9$  kcal mol<sup>-1</sup> via eq 2] is placed between the polarity of methanol [ $E_T(30) = 55.4$  kcal mol<sup>-1</sup>] and water [ $E_T(30) = 63.1$  kcal mol<sup>-1</sup>], whereas the polarity of a MCM-41, synthesized in the presence of a hydrophobic inorganic precursor, ranges between the polarity of dichloromethane [ $E_T(30) = 40.7$  kcal mol<sup>-1</sup>] and 2-propanol [ $E_T(30) = 48.4$  kcal mol<sup>-1</sup>].<sup>4</sup> The value of the  $E_T(30)$  polarity parameter reported for the cavity inside a silica gel, produced by the sol-gel process, is indirectly confirmed by results of Bright et al.,<sup>2</sup> obtained by means of pyrene as a polarity probe inside a similarly synthesized silica gel. With pyrene as fluorescence polarity probe, the intensity ratio  $\mathbf{Py} = I_1/I_3$  of its  $I_1$  and  $I_3$  emission bands at  $\lambda = 375$  and  $384$  nm, respectively, is used as measure of the solvent polarity.  $\mathbf{Py}$  does also correlate with the  $E_T(30)$  solvent parameter. For protic solvents, the following correlation (eq 3) was reported by Dong and Winnik,<sup>6</sup> with correlation coefficient  $r$ , standard deviation  $sd$ , and number of solvents  $n$ :

$$\mathbf{Py} = 0.0584E_T(30) - 1.750 \quad (3)$$

$$r = 0.921 \quad n = 19 \quad sd = 0.28$$

Bright et al. reported a  $\mathbf{Py}$  value of 1.75 for a sol-gel-synthesized silica gel.<sup>2</sup> According to eq 3, that value corresponds to an  $E_T(30)$  value of 59.9. The agreement of this value with the independently obtained results of Ohtaki<sup>1</sup> for the  $E_T(30)$  polarity within a silica gel is excellent.

For solute/solvent interactions, the  $E_T(30)$  as well as the  $\mathbf{Py}$  scale of solvent polarity can be expressed by a multiple LSE (linear solvation energy) relationship using the Kamlet-Taft solvent parameters.<sup>7-9</sup> The fundamental Kamlet-Taft approach describes the manifold influence on a solvent-dependent solute property XYZ under study by means of four terms [ $\alpha$ ,  $\beta$ ,  $\pi^*$ , and the Hildebrand solubility parameter ( $\delta_H$ )] according to eq 4:<sup>7-9</sup>

$$XYZ = (XYZ)_0 + h\delta_H^2 + s(\pi^* + d\delta) + a\alpha + b\beta \quad (4)$$

$(XYZ)_0$  is the solute property of a reference system, e.g., a nonpolar medium or the gas phase,  $\alpha$  describes the HBD (hydrogen-bond donating) ability,  $\beta$  the HBA (hydrogen-bond accepting) ability, and  $\pi^*$  the dipolarity/polarizability of the solvents.  $\delta$  is a polarizability correction term that is 1.0 for aromatic, 0.5 for polyhalogenated, and zero for aliphatic solvents.  $a$ ,  $b$ ,  $s$ ,  $d$ , and  $h$  are solvent-independent coefficients. They reflect the susceptibility of the solute with respect to these properties. For solvent effects on spectra, the  $h\delta_H^2$  term is not of importance.<sup>10</sup>

For 166 well-behaved regular solvents, the following

LSE-eq 5 of the  $E_T(30)$  parameter has been calculated by Marcus:<sup>11</sup>

$$E_T(30) = 31.2 + 15.2\alpha + 11.5\pi^* \quad (a/s = 1.32) \quad (5)$$

$$n = 166 \quad r = 0.979 \quad sd = 1.1$$

For functionalized silicas, Spange and Reuter reported a modified LSE relation for the  $E_T(30)$  parameter.<sup>12</sup>

$$E_T(30)(\text{measured}) = 36.1 + 14.84\alpha + 5.33\pi^* \quad (a/s = 2.7) \quad (6)$$

$$n = 30 \quad r = 0.964 \quad sd = 1.12$$

Equation 6 suggests that the HBD capacity of the silica surface, as measured by  $\alpha$ , contributes stronger to the value of the measured  $E_T(30)$  parameter than in well-behaved regular solvents. The direct determination of the empirical  $E_T(30)$  polarity parameter within ormosils was reported by Avnir et al.<sup>13</sup> The authors incorporated the polarity indicator **1** during a sol-gel process into a methyl group functionalized ormosil network. Then, the  $E_T(30)$  value was determined by measuring the UV/vis absorption maximum of the encapsulated dye **1** according to eq 1. The polarity within the cavities of the functionalized ormosil network was found to be strongly dependent on the composition of the materials and on the polarity of adsorbed liquids used.<sup>13</sup> The  $E_T(30)$  polarity parameter of an ormosil sample containing a small amount of methyl groups (90% TMOS and 10% trimethoxymethylsilane were used for this sample preparation in the sol-gel process) is similar to the surface polarity of bare silica particles, i.e.,  $E_T(30) = 58 \pm 1$  kcal mol<sup>-1</sup>.<sup>12,14,15</sup> However, the determination of the  $E_T(30)$  parameter within a pure, nonorganically modified, silica gel was not reported in ref 13. According to Figure 2 in ref 13 and to an extrapolation to pure silica, the expected value of the  $E_T(30)$  parameter within pure silica gel should amount to  $59.5 \pm 0.2$  kcal mol<sup>-1</sup>. To test this presumption, the  $E_T(30)$  polarity within pure silica gels was checked by employing the same synthetic procedure as reported by Avnir et al. (these experiments will be described later).<sup>13</sup> In all experiments, we have found that encapsulated **1** was protonated within the pure silica gel network and the  $E_T(30)$  value was, therefore, not directly available. Hence, it is expected that the acid strength of the internal silanol groups within a silica gel is larger than those of an external silica surface.

In some recent papers it was shown that the Kamlet-Taft parameters  $\alpha$  and  $\pi^*$  of the external surface of solid materials can be determined by means of two carefully characterized solvatochromic dyes, Fe(phen)<sub>2</sub>(CN)<sub>2</sub> (**2**) and Michler's ketone (**3**) (Scheme 1).<sup>16,17</sup>

(11) Marcus, Y. *Chem. Soc. Rev.* **1993**, 409.

(12) Spange, S.; Reuter, A. *Langmuir* **1999**, 15, 141.

(13) Rottman, C.; Grader, G. S.; Hazan, Y. D.; Avnir, D. *Langmuir* **1996**, 12, 5505.

(14) Spange, S.; Reuter, A.; Vilsmeier, E. *Colloid Polym. Sci.* **1996**, 274, 59.

(15) Taverner, S. J.; Clark, J. H.; Gray, G. W.; Heath, P. A.; Macquarrie, D. J. *J. Chem. Soc., Chem. Commun.* **1997**, 1147.

(16) Spange, S.; Keutel, D. *Justus Liebig's Ann. Chem.* **1992**, 423.

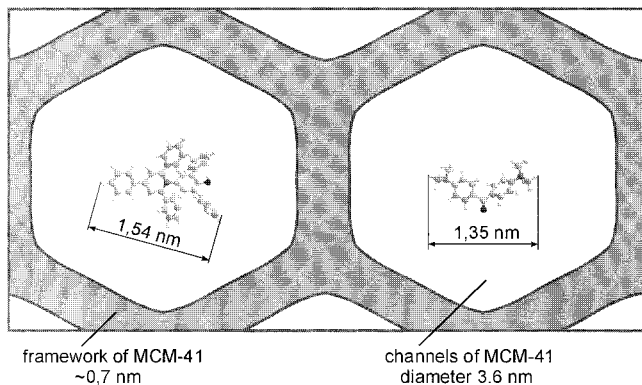
(17) Spange, S.; Keutel, D.; Simon, F. *J. Chim. Phys.* **1992**, 89, 1615-1622.

(6) Dong, D. C.; Winnik, M. A. *Can. J. Chem.* **1984**, 62, 2560.  
(7) Kamlet, M. J.; Abboud, J.-L. M.; Abraham, M. H.; Taft, R. W. *J. Org. Chem.* **1983**, 48, 2877.

(8) Kamlet, M. J.; Hall, T. H.; Boykin, J.; Taft, R. W. *J. Org. Chem.* **1979**, 44, 2599.

(9) Taft, R. W.; Kamlet, M. J. *J. Chem. Soc., Perkin Trans. 2* **1979**, 1723.

(10) Reichardt, C. *Chem. Rev.* **1994**, 94, 2319.

**Scheme 2. Comparison of the Sizes of the Polarity Indicators 1 and 3 with Those of the Framework and Channels of MCM-41**

The solvatochromism of each of these indicators can be well expressed by a specific LSE relationship according to eq 4. **2** serves preferably as an indicator for the HBD capacity  $\alpha$  ( $a/s = 1.37$ ), whereas the shift of the UV/vis absorption maximum of **3** reflects preferably the dipolarity/polarizability  $\pi^*$  ( $a/s = 0.81$ ) of an environment; the coefficients  $b$  and  $d$  are zero for both indicators.<sup>17,18</sup> Therefore, the simultaneous use of the two indicators allows differentiation of contributions of the dipolarity/polarizability and acid/base interactions of a material. As mentioned, for cavities and of solid materials, until now only aggregate polarity values, i.e.,  $E_T(30)$  have been reported<sup>1,2</sup> which involve contributions of both terms  $\alpha$  and  $\pi^*$ . The sizes of the indicators **1–3** do range from 1.35 to 1.54 nm (see Scheme 2); hence, it is expected that their mobility within the channel is not restricted. They can observe the internal polarity of the siliceous frame of MCM-41 as well as the solvent molecules in the channel.

In this paper, we will demonstrate that the UV/vis spectroscopic polarity indicator **3** is equally useful for the distinction between different kinds of acidic silanols within MCM-41. For these measurements, we employed a special technique for recording the UV/vis spectra of the probes within MCM-41 in a temperature range between +35 °C and –80 °C in dichloromethane as solvent. To check the applicability of indicators **2** and **3** to measure reproducibly the polarity of cavities, they were also encapsulated into a silica gel by the sol–gel process with TMOS as silica precursor. By this procedure, an indirect calculation of the  $E_T(30)$  parameter by means of eq 5 or eq 6 is possible as well as a comparison with independently obtained results from ref 1 and 2.

### Experimental Part

**Materials.** The MCM-41 used was kindly presented by Mobil Oil. The MCM-41 was dried carefully by heating it to 400 °C for 24 h with a rate of 1 K/min. The specific surface of MCM-41 was determined to be 753 m<sup>2</sup>/g by the BET method. The pore diameter of this material is exactly 3.6 nm.

The probe dye indicator **1** was kindly given by C. Reichardt, University of Marburg. **2** was prepared according to Schilt.<sup>19</sup>

**3** was purchased from Merck (Darmstadt), recrystallized twice from ethanol, and carefully dried before use.

Dichloromethane and 1,2-dichloroethane were dried over CaH<sub>2</sub> and freshly distilled before use.

2,3-Dihydrofuran (DHF), isobutyl vinyl ether (IBVE), ethyl vinyl ether (EVE), 2-chloroethyl vinyl ether (CIEVE), and cyclohexyl vinyl ether (CHVE) (Aldrich, 99%) were dried over CaH<sub>2</sub>, distilled, and stored under argon.

Poly(4-vinylpyridine) (PVP), with  $M_n = 176\,120$  g/mol and  $M_w/M_n = 1.5$ , was obtained from Polyscience, Inc.

2,6-Di-*tert*-butylpyridine (DTBP) was obtained from Merck and used as received.

**Sol–Gel Process for Synthesizing the Probe Dye Doped Silica Gel Materials.** For the encapsulation of the indicator dyes **1–3** we have used a similar procedure as reported for respective auramine hydrochloride as dye.<sup>20</sup>

The solvatochromic indicator was dissolved in the methanol component before mixing. Tetramethoxysilane (TMOS), methanol, and water were then mixed in the mole ratio 1:4:10 and stirred for 1 h to form a homogeneous and transparent sol. Two different mole ratios ( $10^{-4}$  and  $10^{-6}$  mole) of the dyes **1–3** were tested. The mixture was kept for 24 h at 50 °C. The gel was then dried under vacuum at 80 °C. At higher temperature, decomposition of the encapsulated dye **2** was observed.

**Cationic Polymerization Procedure.** The dried MCM-41 (100 mg) was poured into a flask under argon and immediately covered with 10 mL of dichloromethane. The resulting suspension was shaken for 10 min at the reaction temperature (–25 °C), and the desired amount of monomer was added (50  $\mu$ L to 1.0 mL). After a reaction time of 24 h, the suspension was filtered, and the filter residue was washed three times with 15 mL of dichloromethane. The hybrid materials were dried in high vacuum at 40 °C.

**Solvatochromic Measurements.** For the UV/vis measurements of the MCM-41 slurries in organic solvents, a diode array spectrometer MCS 4 with glass-fiber optics connected with an immersion cuvette TSM 5 A (Carl Zeiss Jena GmbH) was used (see Scheme 3).

The sol–gel-produced silica samples doped with the probe dyes were measured as dried solids in reflectance, using a special device suitable for powders.

**Calculation of the Polarity Parameters.** The solvatochromism and properties of these indicators, as well as the mathematical procedure for the determination of the individual LSE approaches of the indicators, have been already reported in detail.<sup>16,17</sup>

The multiple correlation equations, eqs 7 and 8, were used to separate the respective property  $\alpha$  or  $\pi^*$  from the unit of measurement of each  $\nu_{\max}(\text{indicator})$ :<sup>21</sup>

$$\alpha = -7.900 + 0.453(\nu_{\max}(\mathbf{2}) \times 10^{-3}) + 0.021(\nu_{\max}(\mathbf{3}) \times 10^{-3}) \quad (7)$$

$$r = 0.949 \quad \text{sd} = 0.17$$

$$n = 34 \quad \text{significance } (F) = 0.000$$

$$\pi^* = 13.889 - 0.251(\nu_{\max}(\mathbf{2}) \times 10^{-3}) - 0.320(\nu_{\max}(\mathbf{3}) \times 10^{-3}) \quad (8)$$

$$r = 0.569 \quad \text{sd} = 0.155$$

$$n = 36 \quad F = 0.001$$

The quality of eq 7 is sufficient to examine accurate values of the  $\alpha$  parameter. Despite the poor correlation coefficient of eq 8 in determining  $\pi^*$  values, the significance is sufficient for an estimate. This should be considered by interpreting the results.

(18) Spange, S.; Keutel, D. *Justus Liebigs Ann. Chem.* **1993**, 981–985.

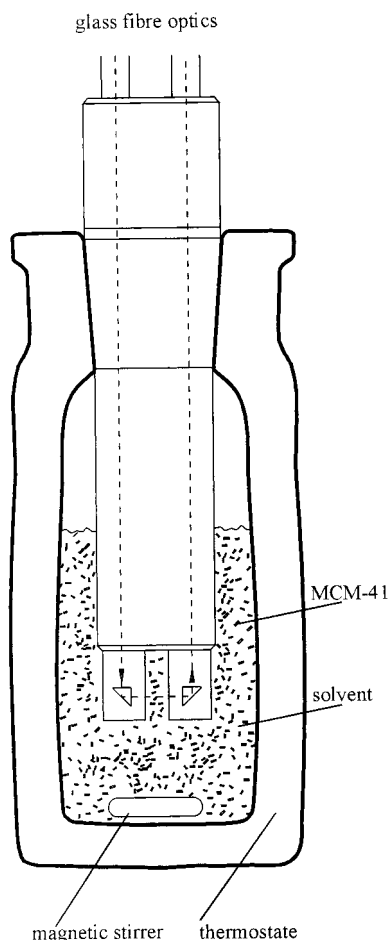
(19) Schilt, A. A. *J. Am. Chem. Soc.* **1960**, 82, 3000.

(20) Tatsumisago, M.; Sakai, Y.; Takashima, H.; Minami, T. *J. Sol-Gel Sci. Technol.* **1997**, 10, 13.

(21) Spange, S.; Vilsmeier, E.; Zimmermann, Y. *J. Phys. Chem. B* **1999**, in preparation.



**Scheme 3. Cell for UV/Vis Measurements with Glass Fiber Optics and Connected with the Immersion Cuvette TSM 5 A (Carl Zeiss Jena GmbH) (Optical Path Length = 0.5 cm)**



**Elemental Analysis.** The quantitative elemental analyses were carried out with Vario EL from the Elementaranalyzen GmbH company.

## Results and Discussion

At first, the two indicators **2** and **3**, respectively, were encapsulated within a silica gel by the sol-gel technique. The colored silicas were measured by two different UV/vis techniques: by reflection spectroscopy of a dried sample and by transmission spectroscopy of the same sample in a 1,2-dichloroethane slurry. For encapsulated **2**, no noticeable difference in the absorption maximum is detectable by comparing the two values:  $\nu_{\max}(\mathbf{2}) = 19\,610\text{ cm}^{-1}$ , measured as dried solid in reflectance, and  $\nu_{\max}(\mathbf{2}) = 19\,560\text{ cm}^{-1}$  as slurry in 1,2-dichloroethane. A concentration dependence of the shift of the absorption maxima of the encapsulated indicators **2** and **3** is not observed. It must be noted, however, that an additional shoulder at about  $\nu_{\max}(\mathbf{2}) = 21\,100\text{ cm}^{-1}$  is observed in the UV/vis spectrum of encapsulated **2**. This indicates that a part of **2** is monoprotonated.<sup>19,22</sup>

For **3** as indicator, a symmetric UV/vis absorption band without shoulders is obtained. The UV/vis absorption maximum of encapsulated **3** in 1,2-dichloroethane suspension is shifted bathochromically [ $\nu_{\max}(\mathbf{3}) = 26\,300$

**Table 1. Values of the Kamlet-Taft Polarity Parameters  $\alpha$  and  $\pi^*$  as Well as Calculated  $E_T(30)$  Polarity Parameters for the Cavities within a Silica Sample Obtained by the Sol-Gel Process from TMOS**

| solid material                             | Kamlet-Taft parameter |         | $E_T(30)$ [kcal mol <sup>-1</sup> ] |      |
|--|-----------------------|---------|-------------------------------------|------|
|  | $\alpha$              | $\pi^*$ | eq 5                                | eq 6 |
| silica gel as dried solid                  | 1.55                  | 0.23    | 59.1                                | 61.2 |
| silica gel as slurry in 1,2-dichloroethane | 1.51                  | 0.56    | 60.1                                | 61.6 |

$\text{cm}^{-1}$ ) as compared to the absorption maximum of **3** measured as dried solid in reflectance [ $\nu_{\max}(\mathbf{3}) = 27\,340\text{ cm}^{-1}$ ]. This indicates the moderately high dipolarity/polarizability of this solvent ( $\pi^* = 0.81$ ),<sup>7</sup> which is evidently detectable by the probe **3**. The corresponding Kamlet-Taft parameters  $\alpha$  and  $\pi^*$  were calculated by eqs 7 and 8 (see Table 1).

When **2** is adsorbed onto the external surface of such a sol-gel-produced silica gel, its UV/vis absorption band appears at  $\nu_{\max}(\mathbf{2}) = 18\,860\text{ cm}^{-1}$ . That would correspond to an  $\alpha$  value of 1.05. This shows that the HBD strength of the external surface of the sol-gel-produced silica is lower than that of the internal surface.

As already mentioned, encapsulation of dye **1** into a silica gel derived from pure TMOS yields a pale-yellow silica gel because the dye becomes protonated [ $\nu_{\max}(\mathbf{1}) = 33\,000\text{ cm}^{-1}$ ] within the silica. This result is not surprising with respect to the rather large  $\alpha$  values of the silica cavities, which can be seen in Table 1. For both sets of experimentally determined  $\pi^*$  and  $\alpha$  values, the corresponding  $E_T(30)$  parameters were calculated by eqs 5 and 6. The agreement of our data with the extrapolated  $E_T(30)$  value of  $59.8\text{ kcal mol}^{-1}$ , according to refs 1 and 2, is excellent. The calculated  $E_T(30)$  values are between  $59.1$  (eq 5) and  $61.6\text{ kcal mol}^{-1}$  (eq 6). The deviation is within the error of the UV/vis measurements. The good agreement of the polarity values measured within a pure silica gel, as obtained by three independent UV/vis spectroscopic probes, supports the correctness of our correlation equations as well as the applicability of the UV/vis technique to measure internal polarities.

For the measurements within MCM-41 materials, we used dichloromethane as liquid, because suspensions of MCM-41 materials are transparent, which allows one to take transmission spectra by means of an immersion cell in the temperature range from  $+35$  to  $-80\text{ }^\circ\text{C}$ .<sup>12</sup>

Figure 1 shows a series of characteristic UV/vis spectra, measured with increasing amounts of adsorbed **2** on MCM-41.

The absorption intensity of adsorbed **2** as function of the total amount of **2** used is shown in Figure 2. The plot approaches the Langmuir adsorption isotherm; the theoretical curve is drawn as solid line:  $\Gamma = \Gamma_{\max}[\chi/(\beta + \chi)]$ , with  $\Gamma$  as surface coverage,  $\Gamma_{\max} = 0.52565$ ,  $\beta = 244.58$ , and  $\chi$  concentration of **2**. The correlation coefficient of the Langmuir plot is  $r = 0.938$ .

In contrast to the UV/vis spectroscopic results obtained from the sol-gel-produced silica gel, an influence of the amount of adsorbed **2** on the position of its UV/vis absorption maximum is observed for MCM-41 as shown in Figure 1. The bathochromic band shift observed is evident and corresponds to a decrease of the measured  $\alpha$  value of the surface from 1.0 to 0.8. Due to the monolayer formation of the adsorbed indicator, it

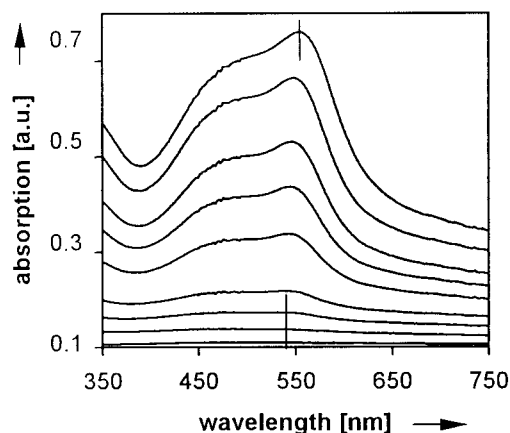


**Figure 1.** UV/vis spectra series of **2** adsorbed to MCM-41 in dichloromethane at 293 K. The concentration of the indicator **2** increases from the bottom to the top (0, 3.7, 11.1, 22.1, 73.7, 140, 258, 442, and 737  $\mu\text{mol}$  of **2**, respectively, per 1 g of MCM-41).

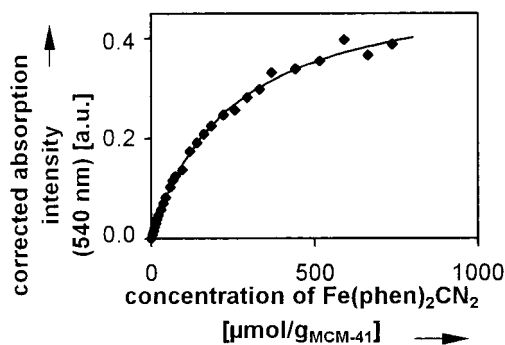


**Figure 2.** Corrected absorption intensity data ( $\blacklozenge$ ) of **2**, adsorbed on the MCM-41 material, as function of the overall concentration of **2**, obtained UV/vis spectroscopically in dichloromethane at 293 K by means of the transmission technique. The corrected absorption intensity is obtained as the difference of the experimentally measured value at  $\lambda_{\text{max}}(\mathbf{2})$  and the intensity of the baseline at  $\lambda(\mathbf{2}) = 700$  nm at each concentration. The solid line is the theoretically calculated curve for the Langmuir isotherm plot.

is obvious that **2** is adsorbed on sites of different acidity. With increasing concentration of **2**, the measured<sup>12</sup> average acidity seems to be decreased. At first, small amounts of **2** are adsorbed to the most acidic sites, corresponding to a minimum of free energy. Due to the distribution of acidity within MCM-41, a further increase of the concentration of **2** is responsible for the observed bathochromic band shift.

Dye **3**, when adsorbed to the channels of MCM-41 shows, surprisingly, two UV/vis absorption maxima in the visible region as shown in Figure 3.

The absorption at  $\lambda_{\text{max}} = 398$  nm is expected and relates well to the dipolarity/polarizability of the silanol group environment, as reported for several other silica samples.<sup>12,14</sup> The other absorption of **3** at  $\lambda_{\text{max}} = 486$  nm, when adsorbed to a solid, is rather unexpected for bare silicas. This UV/vis absorption band does not appear when **3** is adsorbed to common silica samples such as Aerosil 300, KG 60 (Merck), or the sol-gel-produced silica.<sup>12,14</sup> The new absorption band at  $\lambda_{\text{max}} = 486$  nm, derived from **3**, is attributed to an oxonium  $[4-(\text{CH}_3)_2\text{N}(\text{C}_6\text{H}_4)]_2\text{C}^+\text{O}^-$  surface species.<sup>21</sup> Generally, the appearance of the oxonium species of **3** is caused by a selective complexation of the carbonyl oxygen with

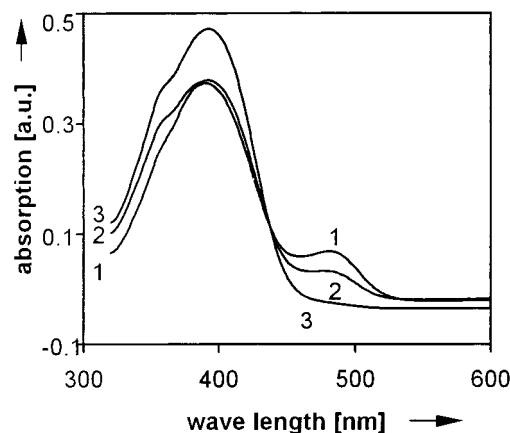


**Figure 3.** UV/vis absorption spectra of **3** adsorbed to MCM-41 in dichloromethane at 293 K ( $1 \times 10^{-6}$  mol of **3** was adsorbed to 0.102 g of MCM-41): spectrum 1, without DTBP; spectrum 2, titrated with  $2.35 \times 10^{-5}$  mol DTBP; and spectrum 3, titrated with  $4.70 \times 10^{-4}$  mol DTBP

a strong acid.<sup>16,23</sup> The same effect is observed when **3** is adsorbed to alumina surfaces.<sup>21</sup> Therefore, either mobile protons or Lewis acid sites within the MCM-41 channels are responsible for this effect. To distinguish between Brønsted and Lewis acidic sites, a titration of the suspension with the sterically hindered base 2,6-di-*tert*-butylpyridine (DTBP) was achieved. As seen in the UV/vis spectra, the absorption band of **3** on MCM-41 at  $\lambda_{\text{max}} = 486$  nm successively disappears when DTBP is added. In contrast, the absorption band behaves invariable on alumina or some aluminosilicates when titrated with DTBP.<sup>21</sup> This comparison shows that additional acidic *mobile protons* are present in the channels of MCM-41 (Scheme 4). The shoulder appearing at  $\lambda_{\text{max}} = 360$  nm in the UV/vis spectra of **3** is caused when **3** is desorbed into the surrounding solution phase.

The presence of three qualitatively different silanol environments was also observed in the IR spectra of siliceous MCM-41.<sup>24,25</sup> We suggest that the internal silanol groups of MCM-41 show a wider polarity distribution than those of external surfaces of common silica materials.

The detection of the rather acidic mobile protons within MCM-41 by means of **3** as polarity indicator is consistent with the observation that MCM-41 can directly initiate the cationic host-guest polymerization of electron-rich monomers such as vinyl ethers or *N*-vinylcarbazole (see Table 2). Consequently, the cationic polymerization of vinyl ethers within MCM-41 is drastically suppressed in the presence of **3**, because the electrophilicity of the  $[4-(\text{CH}_3)_2\text{NC}_6\text{H}_4]_2\text{C}^+\text{O}^-$  surface species (**3**<sup>+</sup>) is low.<sup>26</sup> The mechanism of cationic host-guest polymerizations and the polymer structures formed in MCM-41 will be reported in a further paper.<sup>27</sup>

The external surface of the sol-gel-produced silica does not directly initiate the cationic polymerization of vinyl ethers.

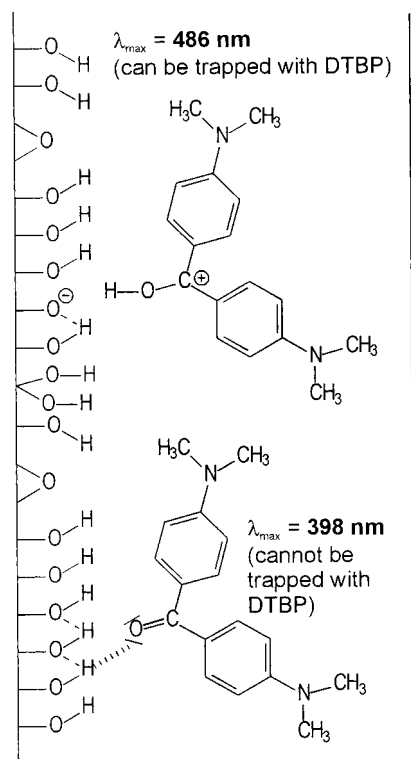
(23) Spange, S.; Vilsmeier, E.; Adolph, S.; Faehrmann, A. *J. Phys. Org. Chem.* **1999**, *12*, 547.

(24) Chen, J.; Li, Q.; Xu, R.; Xiao, F. *Angew. Chem.* **1995**, *107*, 2898; *Angew. Chem., Int. Ed. Engl.* **1995**, *34*, 2898.

(25) Jentys, A.; Pham, N. H.; Vinek, H. *J. Chem. Soc., Faraday Trans.* **1996**, *92*, 3287.

(26) The electrophilicity of **3**<sup>+</sup> was estimated using structurally similar compounds: Mayr, H.; Patz, M. *Angew. Chem.* **1994**, *106*, 990; *Angew. Chem. Int. Ed. Engl.* **1994**, *33*, 938.

(27) Spange, S.; Graeser, A.; Rehak, P.; Jaeger, C.; Schulz, M. *Macromol. Chem. Rapid Commun.* **1999**, in press.

**Scheme 4. The Two Different Structures of **3** Adsorbed to the Silanol Groups within the Channel of MCM-41****Table 2. Catalytic Activity of MCM-41 for Cationic Host–Guest Polymerization of Vinyl Monomers<sup>a</sup>**

| monomer                    | reaction temp [°C] | $n/m$<br>$10^{-3}[\text{mol/g}]^b$ | carbon content <sup>c</sup><br>[%] | yield [%]<br>soluble polymer | hybrid material |
|----------------------------|--------------------|------------------------------------|------------------------------------|------------------------------|-----------------|
| DHF                        | -78                | 82.95                              | 5.1                                | 0.1                          | 1.3             |
| DHF                        | -25                | 87.70                              | 18.1                               | 0.3                          | 4.3             |
| EVE                        | -25                | 92.04                              | 17.6                               | 5.3                          | 4.0             |
| EVE/ <b>3</b> <sup>d</sup> | -25                | 51.06                              | 2.8                                | 11.4                         | 1.2             |
| IBVE                       | -25                | 62.50                              | 6.5                                | 2.4                          | 1.5             |
| CHVE                       | -25                | 1.17                               | 4.0                                | 30.3                         | 35.0            |
| CHVE                       | -25                | 14.01                              | 14.7                               | 7.1                          | 10.9            |
| CHVE                       | -25                | 62.09                              | 19.6                               | 17.7                         | 3.3             |
| NVC                        | -25                | 28.96                              | 30.2                               | 67.5                         | 6.2             |

<sup>a</sup> The solvent used was dichloromethane and the reaction time was 24 h. <sup>b</sup> Ratio ( $n$  is the amount of monomer used;  $m$  is the mass of MCM-41). <sup>c</sup> Of the MCM-41 hybrid material. <sup>d</sup> A total of  $10^{-6}$  mol of **3** to 100 mg of MCM-41. The intensity of the oxonium absorption in the UV/vis spectrum at  $\lambda_{\text{max}} = 495$  nm remains stable in the presence of vinyl ethers.

Whereas the UV/vis absorption maximum of **2**, adsorbed to MCM-41 is a function of the concentration of **2**, the position of the UV/vis absorption maximum of adsorbed **3** at  $\lambda_{\text{max}} = 398$  nm is concentration-independent. This result shows that **2** measures an average polarity of both acidic sites. It should be noted that the protonated form of **2**, detectable as a shoulder in the UV/vis spectrum as mentioned for the sol–gel-produced silica, is not observed on MCM-41 (see also the series of spectra in Figure 1). This result shows that the rigidity of the sol–gel-produced silica glass also has an influence on the structure of the encapsulated indicators.

By using the  $\nu_{\text{max}}$  values of **2** and **3**, the corresponding  $\alpha$  and  $\pi^*$  values of MCM-41 as function of the concentration of **2** can be principally calculated. Then, by using eqs 7 and 8, independent  $E_{\text{T}}(30)$  values can be calcu-

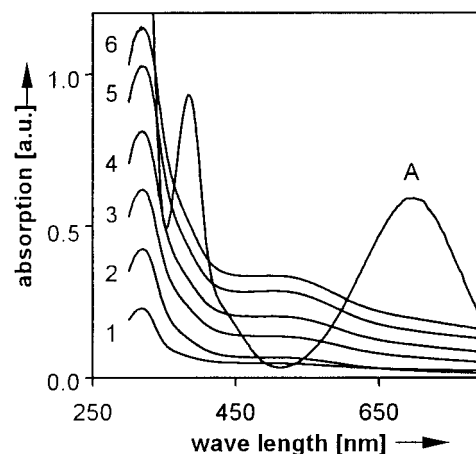


**Figure 4.** UV/vis absorption spectra of Reichardt's dye **1** adsorbed to MCM-41 in dichloromethane at 293 K. The concentrations of the dye are 1.87  $\mu\text{mol}$  (1), 5.6  $\mu\text{mol}$  (2), 9.33  $\mu\text{mol}$  (3), 13.1  $\mu\text{mol}$  (4), 18.7  $\mu\text{mol}$  (5), and 26.7  $\mu\text{mol}$  (6). Spectrum A is a typical spectrum of the dye in the former dichloromethane solution, which contains small amounts of protons from HCl traces.

lated. Values of  $E_{\text{T}}(30)$  for MCM-41 are expected to lie between 59.9 (eq 5) and 57.4  $\text{kcal mol}^{-1}$  (eq 6). Despite the presence of low amounts of acidic protons within MCM-41, Reichardt's dye **1** was suitable to determine directly the value of the  $E_{\text{T}}(30)$  parameter. A series of characteristic UV/vis spectra of dye **1**, adsorbed with different concentration on MCM-41 is shown in Figure 4.

The UV/vis spectra of dye **1** adsorbed on MCM-41 are rather broad, indicating that the surface polarity shows a wide distribution. Also the protonated form of the dye **1** is detectable by the shoulder at about  $\lambda = 380$  nm. The addition of the polymeric base PVP to dye **1** adsorbed on MCM-41 does not influence its UV/vis spectrum. That is an indication that dye **1** is located within the channels because the PVP cannot immediately penetrate into the nanopores of MCM-41. The influence of the concentration of dye **1** upon the position of the visible absorption maximum is not as large as observed for **2** as surface polarity indicator. However, the value of the  $E_{\text{T}}(30)$  parameter, utilized at the absorption maximum of **1**, amounts to 57.5 (low concentration of **1**) and 55.9 (higher concentration of **1**)  $\text{kcal mol}^{-1}$ . The agreement with the  $E_{\text{T}}(30)$  values predicted by eq 6, using the  $\alpha$  and  $\pi^*$  values obtained by the  $\nu_{\text{max}}$  values of probes **2** and **3**, is excellent. Thus, the LSE equation for the  $E_{\text{T}}(30)$  parameter, derived from functionalized silicas, also gives a better agreement between measured and calculated data. These results hint at the fact that the hydrogen-bond acidity within the MCM-41 also contributes stronger to the measurable  $E_{\text{T}}(30)$  polarity than does the dipolarity/polarizability.

We assume that the influence of concentration of the probe dyes upon the change of the  $\nu_{\text{max}}$  value of the probes depends on the quotient of the susceptibilities ( $a/s$ ) of the  $\alpha$  to the  $\pi^*$  term according to the behavior of the indicators in well-behaved regular solvents. It increases in the order: **2** ( $a/s = 1.37$ ) > **1** ( $a/s = 1.32$ ) > **3** ( $a/s = 0.81$ ). This indicates that the surface acidity distribution can be measured as a function of probe concentration, but the dipolarity/dipolarizability seems to be a rather constant quantity, independent of the concentration of **3**. To support this presumption, an



**Table 3. Influence of Temperature on the Value of the Kamlet–Taft Parameters  $\alpha$  and  $\pi^*$ , as Well as the  $E_T(30)$  Values Measuring the Internal Polarity of MCM-41 in Dichloromethane**

| $T$ [K] | $\nu_{\max}$<br>[ $10^{-3} \text{ cm}^{-1}$ ] |       | $\alpha$ | $\pi^*$ | $E_T(30)$<br>[kcal mol $^{-1}$ ] |      |
|---------|---|-------|----------|---------|----------------------------------|------|
|         | 2   | 3     |          |         | eq 5                             | eq 6 |
| 308     | 18.55   | 25.25 | 1.04     | 1.15    | 60.2                             | 58.3 |
| 303     | 18.55   | 25.25 | 1.04     | 1.15    | 60.2                             | 58.3 |
| 298     | 18.55   | 25.25 | 1.04     | 1.15    | 60.2                             | 58.3 |
| 293     | 18.52   | 25.32 | 1.02     | 1.14    | 59.8                             | 58.0 |
| 283     | 18.55   | 25.13 | 1.03     | 1.19    | 60.6                             | 58.5 |
| 273     | 18.59   | 25.13 | 1.05     | 1.18    | 60.7                             | 58.7 |
| 263     | 18.59   | 25.25 | 1.05     | 1.14    | 60.3                             | 58.5 |
| 253     | 18.62   | 25.13 | 1.06     | 1.17    | 60.9                             | 59.0 |
| 243     | 18.62   | 25.06 | 1.06     | 1.19    | 61.1                             | 59.1 |
| 233     | 18.69   | 25.06 | 1.09     | 1.18    | 61.4                             | 59.5 |
| 223     | 18.73   | 25.06 | 1.11     | 1.17    | 61.5                             | 59.7 |
| 213     | 18.76   | 25.00 | 1.12     | 1.18    | 61.8                             | 60.0 |

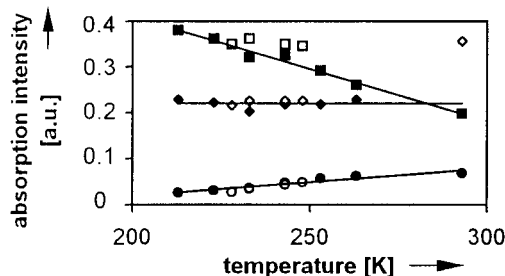


**Figure 5.** Influence of the temperature on the absorption intensity of the two absorption maxima of **3** on MCM-41 [(■, □) at  $\lambda = 398$  nm and (●, ○) at  $\lambda = 486$  nm] and on that of the surrounding solution phase [(◆, ◇) at  $\lambda = 360$  nm]. The filled points correspond to data measured during the cooling and the open points to those of the heating process.

influence of the temperature upon the effective surface polarity is also expected, according to results on internal polarity of frozen glasses from the literature.<sup>28</sup> It should be noted that the external surface polarity of silica nanoparticles (Aerosil 300) suspended in dichloromethane is temperature-independent in the temperature range from +20 to  $-78$  °C.<sup>12</sup> Table 3 summarizes the temperature-dependent results for **2** and **3** as polarity indicators, measured on MCM-41 suspended in dichloromethane in the temperature range between +35 and  $-60$  °C.

With decreasing temperature, the surface acidity increases significantly as measured by probe **2**.

As expected, the position of the absorption band of **3** at  $\lambda_{\max} = 398$  nm, when adsorbed to MCM-41, is rather temperature-independent. The other absorption band of **3** at  $\lambda_{\max} = 482$  nm (20 °C) shifts to  $\lambda_{\max} = 489$  nm ( $-60$  °C). This small bathochromic UV/vis band shift<sup>23</sup> also indicates an increase of the acidity of the mobile protons within the channels. Because the acidity is influenced by the temperature, the absorption intensities of the two UV/vis absorption bands of adsorbed **3** are also changed. This is shown in Figure 5.

Therefore, both the strength and the concentration of the hydrogen-bond acidic sites are influenced by the temperature. The calculated Kamlet–Taft parameters  $\alpha$  and  $\pi^*$  of MCM-41 as function of temperature are shown in Figure 6.

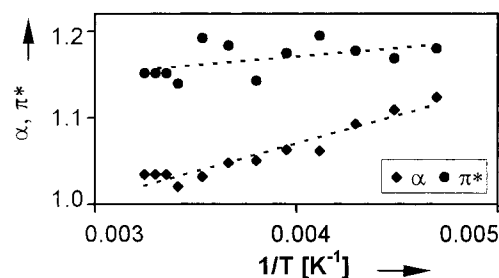


**Figure 6.** Influence of the temperature on the average value of the dipolarity/polarizability ( $\pi^*$ , ●) and hydrogen-bond acidity ( $\alpha$ , ◆) of MCM-41 in dichloromethane.

With decreasing temperature, the indicator **2** measures a larger acidity because it is stronger adsorbed. The dipolarity/polarizability interaction, however, seems to be temperature-independent. This result is consistent with the isokinetic behavior of the polarity, obtained for several groups of solvents.<sup>29</sup> The intermolecular interactions between the surface of a cavity and an encapsulated solvatochromic probe dye<sup>30</sup> is analogous (or similar) to the intermolecular solute/solvent interaction between a dissolved probe dye and the surrounding solvation shell.

So far, there is a lack of suitable indicators for the determination of the  $\beta$  parameter of highly acidic materials.<sup>31</sup> However, it is assumed that the value of the  $\beta$  parameter only scarcely contributes to the  $E_T(30)$  value of solid acids.<sup>12,23</sup>

## Conclusion

The hydrogen-bond-donating acidity and dipolarity/polarizability of surfaces inside sol–gel-produced silica gel and MCM-41 can be gradually analyzed by means of dyes **2** and **3** as suitable polarity indicators for siliceous materials. The correctness of the determined  $\alpha$  and  $\pi^*$  values is tested by means of specific LSE correlations with independently calculated  $E_T(30)$  polarity parameters according to:  $E_T(30) = f(\alpha, \pi^*)$ .

Dye **3** is also suitable for the detection of surface environments of different acidity, because two different UV/vis absorption maxima can be observed which are caused by two differently acidic silanol surface groups on MCM-41. The surface acidity as measured by dye **3** correlates well with the catalytic activity of MCM-41 in initiating the host–guest cationic polymerization of electron-rich vinyl monomers, e.g., vinyl ethers and *N*-vinylcarbazole.

**Acknowledgment.** Financial support for this project, in particular by the Deutsche Forschungsgemeinschaft, Bonn, and the Fonds der Chemischen Industrie, Frankfurt/Main, is gratefully acknowledged. We thank Mobil Oil for the gift of the excellent MCM-41 material. We thank Christine Schmidt for the preparation of the silica gel materials doped with probe dyes.

CM990308T

(28) Bublit, G. U.; Boxer, S. G. *J. Am. Chem. Soc.* **1998**, *120*, 3988 and references therein.

(29) Linert, W.; Jameson, R. F. *J. Chem. Soc., Perkin Trans.* **1993**, *2*, 1415.

(30) Meinershagen, J. L.; Bein, A. *J. Am. Chem. Soc.* **1999**, *121*, 448.

(31) Spange, S.; Reuter, A.; Linert, W. *Langmuir* **1998**, *14*, 3479.